Electronic Supplementary Material (ESI) for Physical Chemistry Chemical Physics.

Atomistic simulations of bulk heterojunctions to evaluate the structural and packing properties of new predicted donors in OPVs

Andrés F. Marmolejo-Valencia, Zaahel Mata-Pinzón, Laura Domínguez-Dueñas, and Carlos Amador-Bedolla

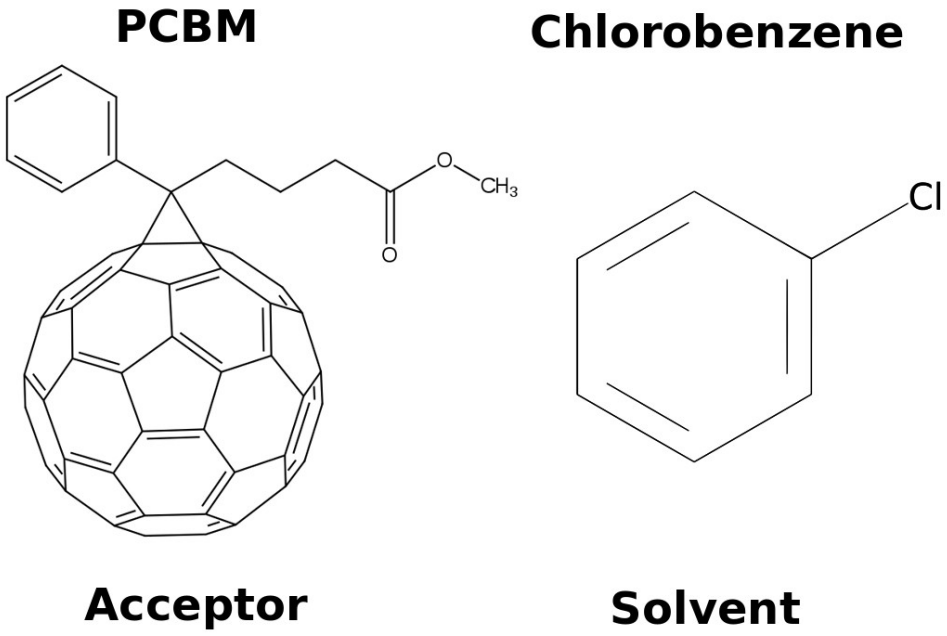

Figure 1S. Structures of electron acceptor PCBM ([6,6]-phenyl-C61-butyric acid methyl ester) and solvent chlorobenzene.

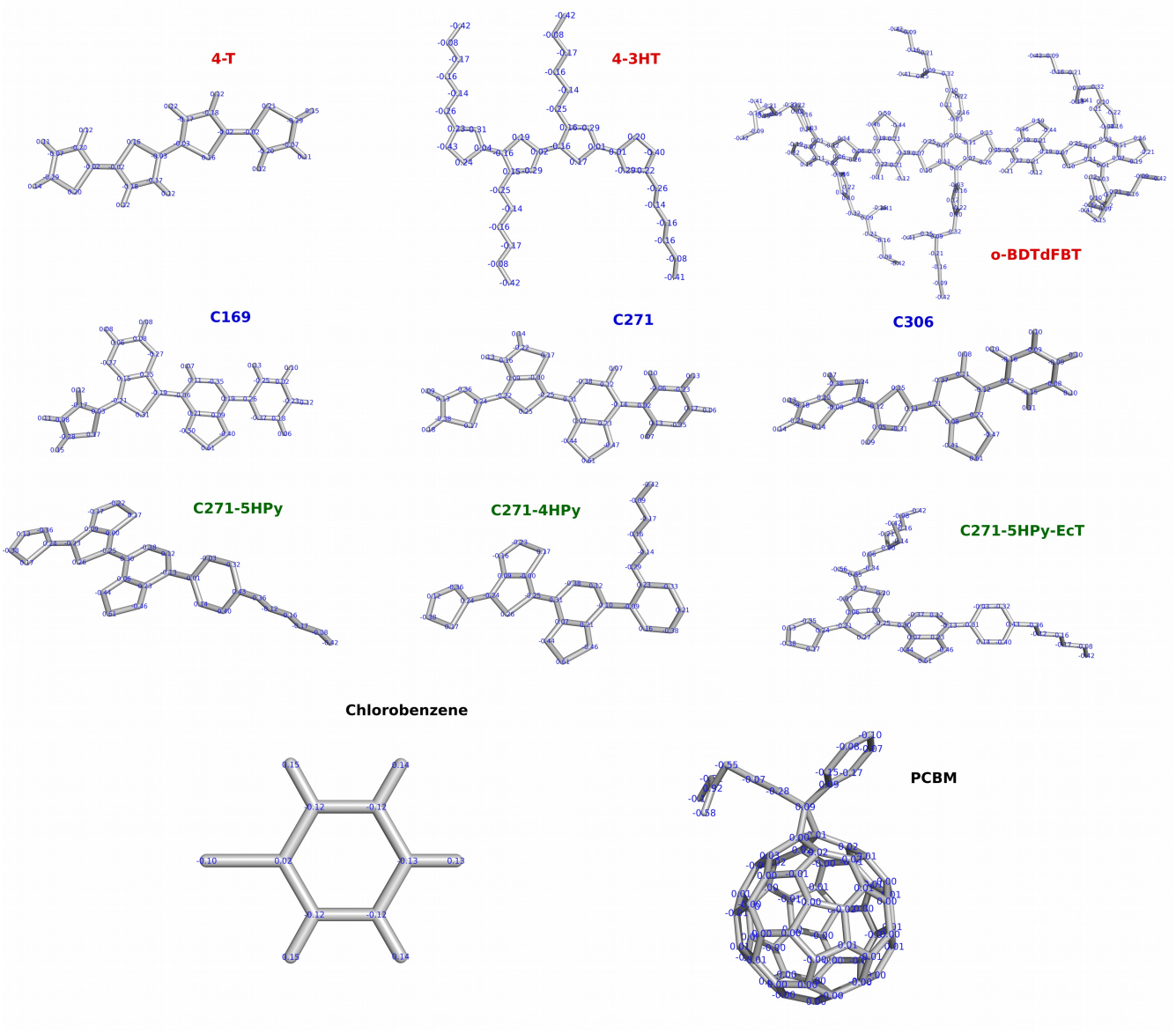

Figure 2S. H-Iter charges calculated for all molecules in the work. The hydrogen atoms were suppressed when side-chains were present.

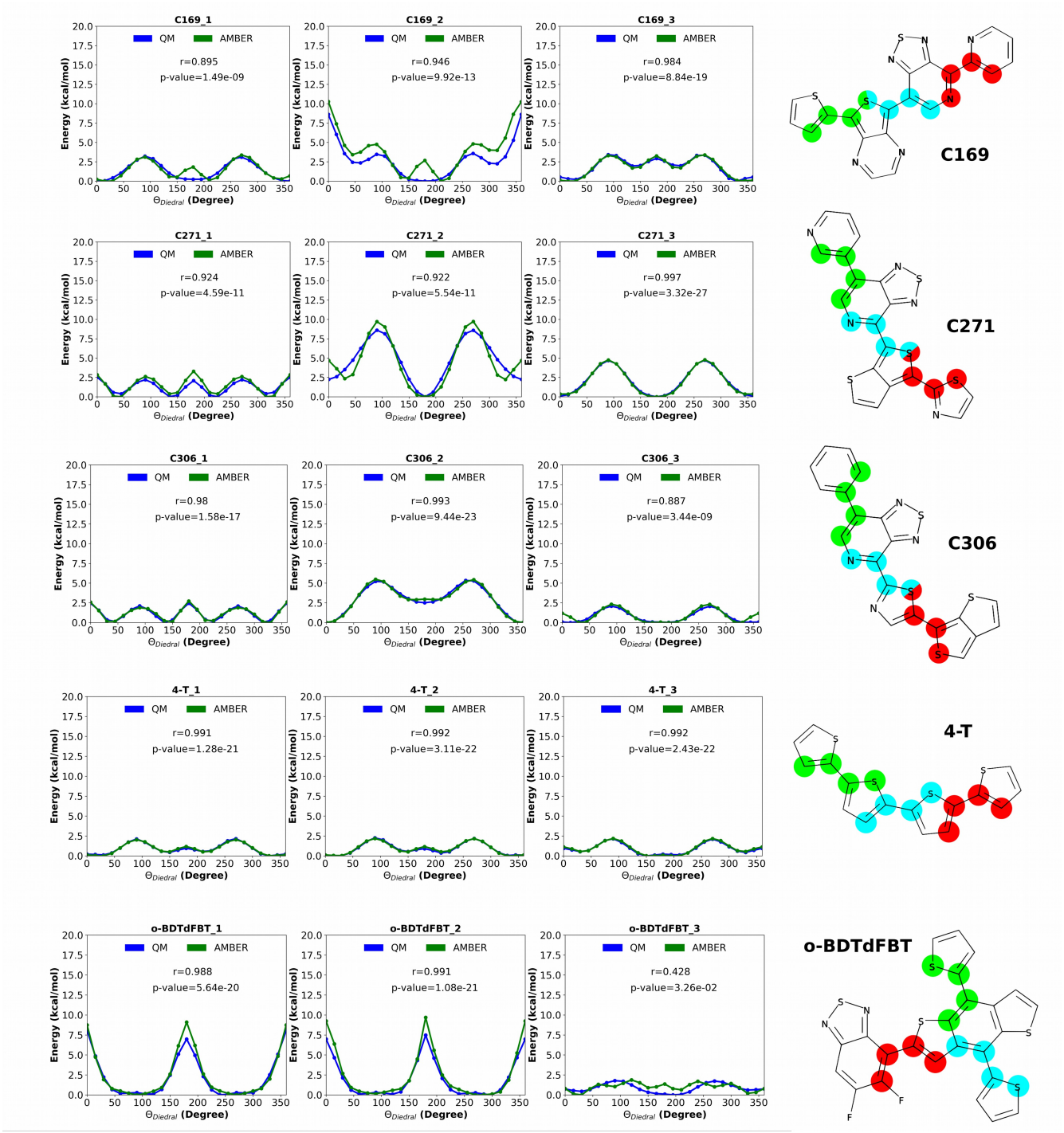

Figure 3S. Rotational barrier fitted for the molecular mechanic representation (AMBER) through dihedral parametrizations of all dihedral paths envolved in rotatable bonds. Paths colored in green, cyan, and red represent the dihedrals selected in the illustrated rotational barriers 1, 2 and 3, respectively. QM was the reference value (cc-TZVP/ω-B97XD). Correlation coefficients and p-values of Pearson were measured too. In the third rotational barrier of 4-T, the path selection does the curves dephased by 180°.

Optimization of dihedral parameters for the atomistic molecular dynamic simulations. Reference torsional barriers were estimated by structural optimizations (Figure 3S) doing dihedral restrictions. Angle values of restricted dihedrals were previously calculated by free optimizations. A dihedral path was selected and sampled every 15 degrees in a range of 0 to 360, while the others dihedral angles (on rotatable bonds) were restricted. Density Functional Theory (DFT) was implemented by using cc-pVTZ basis set and ω-B97XD functional in the Q-Chem4.0 package.

For the force filed GAFF, all of the dihedral potentials over rotatable bonds were turn off and harmonic potential restrictions took control of these dihedrals by fixing the angle values as the quantum reference predicted. Thus, the same angle sampling was carried out by energy minimizations with 30000 steps of steepest descent algorithm in vacuo. An energetic torsional profile was obtained to be optimized later.

Molecular Mechanic dihedral profiles were optimized by genetic algorithm optimizations,[1] that evolved the input data to find maximal similitude against QM profile, adding values of potential (*Vdihedral*) to the total energy calculated above,

$$V_{dihedral} = \frac{k_1}{IDIVF}\left(1+\cos\left(n_1\theta-\gamma_1\right)\right)+\frac{k_2}{IDIVF}\left(1+\cos\left(n_2\theta-\gamma_2\right)\right)$$

and taking the best six dihedral parameters *k1*, *k2*, *n1*, *n2*, *γ1* and *γ2*. To construct the genetic algorithm was required the pyevolve module on python, implementing the tournament selector, 30000 generations, crossover rate of 0.7 and exclusion of elitism. The new energetic profiles were verified turning on the new dihedral parameters and calculating the torsional barriers again (Figure 3S).

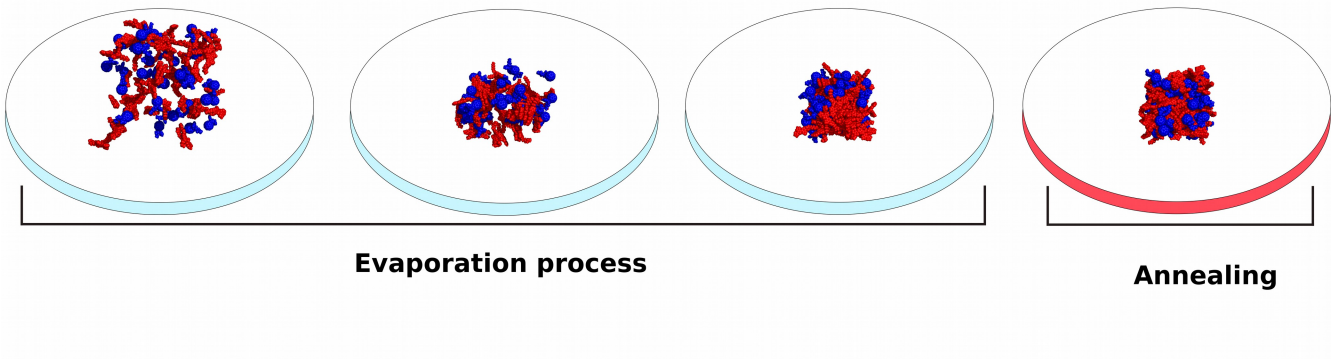

Figure 4S. Illustration of the evaporation process where explicit solvent molecules of chlorobenzene were removed in consecutive steps (the blue plates). Changes after the annealing treatment in the BHJ phase (the red plate). Donor molecules were colored in red, while acceptor molecules colored in blue. Solvent molecules were not drawn in the evaporation for better representation.

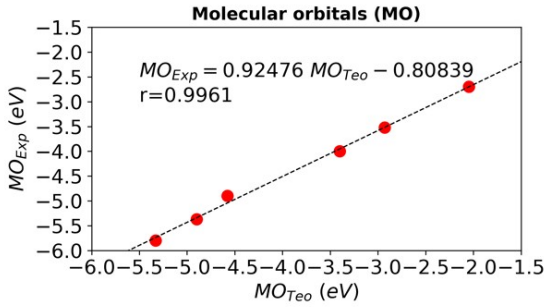

	Frontier Orbitals	MO_{Teo}	MO_{Exp}
PCBM	*HOMO* *LUMO*	-5.33 -3.40	-5.8 -4.0
o-BDT-dFBT	*HOMO* *LUMO*	-4.90 -2.93	-5.37 -3.52
4-3HT	*HOMO* *LUMO*	-4.58 * -2.05**	-4.9 -2.7

* HOMO corrected by shorter chain length used.
**LUMO corrected due to shorter chain length.

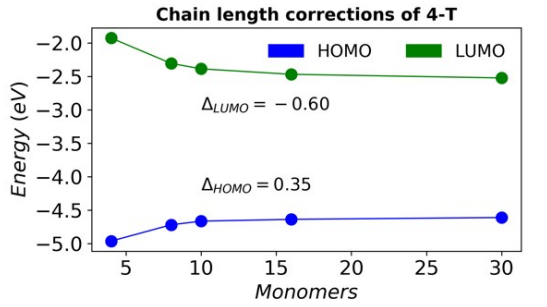

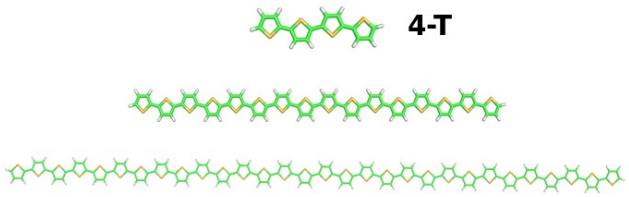

Figure 5S. Linear regression between theoretical molecular orbitals (MO_{Teo}) and experimental molecular orbital (MO_{Exp}). [2,3] MO_{Teo} was an average value calculated by weighted histograms (HOMO or LUMO), for all possible pairs donor-donor and acceptor-acceptor (PCBM$^{o\text{-BDTdFBT}}$, PCBM$^{4\text{-3HT}}$, 4-3HT and o-BDTdFBT) using 6-31G(d,p)/B3LYP DFT theory. PCBM was averaged from PCBM$^{o\text{-BDTdFBT}}$ and PCBM$^{4\text{-3HT}}$. Notice that 4-3HT required corrections of monomer length.

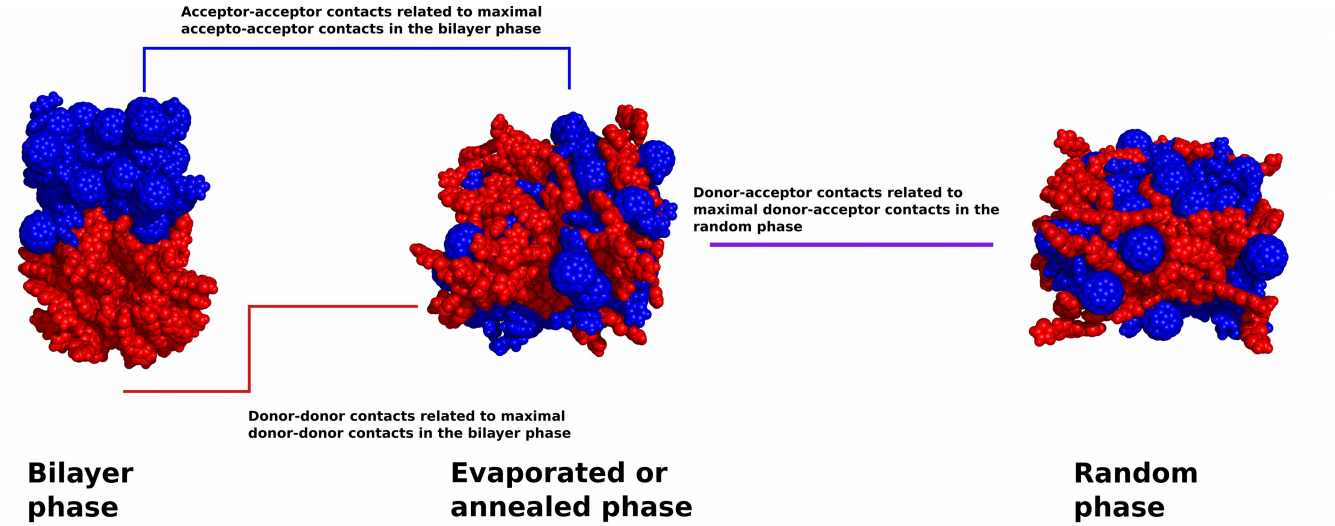

Figure 6S. Bilayer and random phases simulations simulated to calculate the maximal contacts between donor-donor, acceptor-acceptor and donor-acceptor molecules, to normalize the total contacts of evaporated and annealed phases. Donors were colored in red, whereas acceptors were in blue.

Simulations of the bilayer and random phases. First, the bilayer was built inserting fullerene molecules in the minimum cube box that could contain them, the area of this cube was the reference to place donors into a second box, depending on donor type, height was variated. For random phases, donors and acceptors were inserted into a cube box searching the minimal edge length possible. All systems were generated using packmol[4] version 16.344. Simulation parameters were similar to simulations described in the main text. The simulation processes proceed with energy minimizations, later the temperature was equilibrated to 300 K (NVT, 800 ps) and pressure fixed to 1 bar into an isotropic scheme (NPT, 200 ps) and 40 ns of production were simulated. Maximum of contacts for D-D or A-A was estimated from MD bilayer phases, whereas for D-A were provided by MD random phases. Contacts of D-D and A-A couples were divided by two due to double counting.[5]

Table 1S. Frontier orbital levels for donor-donor adduct pairs extracted from annealed BHJ phases, that are a blending of small molecules (donor) and PCBM (acceptor).

Donor	$HOMO_{DD}$ (eV)	$LUMO_{DD}$ (eV)	gap_{DD} (eV)
	Thermal annealing		
C169	-5.44±0.10	-3.70±0.08	1.74±0.16
C271	-5.66±0.11	-3.75±0.09	1.92±0.11
C306	-5.64±0.09	-3.63±0.10	2.02±0.14
4-T	-4.94±0.09	-3.11±0.08	1.87±0.17
4-3HT	-5.04±0.14	-2.74±0.15	2.46±0.31
C271-5HPy	-5.60±0.08	-3.68±0.06	1.91±0.13
C271-4HPy	-5.66±0.09	-3.71±0.10	1.94±0.14
C271-5HPy-EcT	-5.73±0.12	-3.76±0.11	1.96±0.11
o-BDTdFBT	-5.35±0.08	-3.48±0.07	1.87±0.16

Table 2S. Frontier orbitals of acceptor-acceptor phases extracted from evaporated and annealed BHJs, the small molecules (oligomers) were the donors and the PCBM molecule was the acceptor.

Acceptor	$HOMO_{AA}$ (eV)	$LUMO_{AA}$ (eV)	gap_{AA} (eV)
	Evaporation process		
$PCBM^{C169}$	-5.75±0.08	-3.93±0.05	1.83±0.12
$PCBM^{C271}$	-5.74±0.07	-3.93±0.08	1.8±0.07
$PCBM^{C306}$	-5.73±0.06	-3.95±0.07	1.79±0.07
$PCBM^{4\text{-}T}$	-5.73±0.08	-3.95±0.08	1,80±0.09
$PCBM^{4\text{-}3HT}$	-5.73±0.06	-3.94±0.10	1.82±0.08
$PCBM^{C271\text{-}5HPy}$	-5.76±0.04	-3.93±0.08	1.81±0.08
$PCBM^{C271\text{-}4HPy}$	-5.74±0.05	-3.92±0.06	1.82±0.07
$PCBM^{C271\text{-}5HPy\text{-}EcT}$	-5.73±0.05	-3.93±0.08	1.79±0.10
$PCBM^{o\text{-}BDTdFBT}$	-5.74±0.08	-3.94±0.09	1.80±0.07
	Thermal annealing		
$PCBM^{C169}$	-5.74±0.09	-3.93±0.06	1.81±0.07
$PCBM^{C271}$	-5.75±0.06	-3.93±0.06	1.81±0.08
$PCBM^{C306}$	-5.73±0.07	-3.94±0.04	1.79±0.07
$PCBM^{4\text{-}T}$	-5.73±0.08	-3.93±0.08	1.80±0.10
$PCBM^{4\text{-}3HT}$	-5.75±0.05	-3.95±0.06	1.79±0.12
$PCBM^{C271\text{-}5HPy}$	-5.77±0.06	-3.94±0.06	1.83±0.07
$PCBM^{C271\text{-}4HPy}$	-5.76±0.06	-3.95±0.10	1.81±0.08
$PCBM^{C271\text{-}5HPy\text{-}EcT}$	-5.76±0.07	-3.92±0.07	1.83±0.05
$PCBM^{o\text{-}BDTdFBT}$	-5.76±0.06	-3.95±0.1	1.81±0.07

References

1. K.M. García-Ruiz, A. F. Marmolejo-Valencia, González-Navejas, L. Dominguez, C. Amador-Bedolla. *J .Mol. Model.* 2019 25, 110.
2. W. C. Tsoi, S. J. Spencer, L. Yang, A. M. Ballantyne, P. G. Nicholson, A. Turnbull, A. G. Shard, C. E. Murphy, D. D. C. Bradley, J. Nelson and J.-S. Kim, *Macromolecules*, 2011, 44, 2944–2952.
3. L. Yuan, Y. Zhao, J. Zhang, Y. Zhang, L. Zhu, K. Lu, W. Yan and Z. Wei, *Adv. Mater.*, 2015, 27, 4229–4233.
4. L. Martínez, R. Andrade, E. G. Birgin, J. M. Martínez. *J. Comput. Chem.*, 2009, 30,2157-2164.
5. R. Alessandri, J. J. Uusitalo, A. H. de Vries, R. W. A. Havenith and S. J. Marrink, *J. Am. Chem. Soc.*, 2017, 139, 3697–3705.